Available online at www.sciencedirect.com
ScienceDirect
International Journal of Thermal Sciences 48 (2009) 412–420
International Journal of Thermal Sciences
www.elsevier.com/locate/ijts

Numerical study of the solidification of successive thick metal layers

Cédric Le Bot *, Eric Arquis

University Bordeaux 1, Laboratory TREFLE, 16 Avenue Pey Berland, 33607 Pessac Cedex, France

Received 16 October 2007; received in revised form 16 July 2008; accepted 8 August 2008

Available online 12 September 2008

Abstract

Impact and solidification of droplets onto a dry solid substrate generates thin or thick substrates depending on size, velocity and physical properties of the fluid particles (during spray or deposition, for example). Numerous and complex phenomena occur in such processes. Difficulties are due to a lack of control of the resulting film, since fluid dynamics (due to droplets impact, for example) heat transfer and solidification interact and influence the final shape and properties of the film.

This paper proposes the numerical study of the influence of some material properties upon the manufacturing of a thick coating. For this purpose, a simplified 1D model is used to simulate "deposition" and solidification of successive metal layers upon an initially cold substrate, assuming that there is no fluid flow. Then, the influence of several parameters is studied: layers thickness, initial substrate and layers temperatures, thermal contact resistance between two elements (substrate or layer) and impact frequency.

Keywords: Solidification; Thermal contact resistance; Impact frequency; Numerical modelling

1. Introduction

Coating manufacturing is a process often used to cover a substrate with a thin or thick metallic film by thermal spray or deposition. Fluid droplets reach the cold substrate, spread onto it and freeze. Interactions between droplets alter cooling and solidification rates and subsequent properties of the coating. The structure of the final coating remains difficult to predict because of the random character of droplets impacts in terms of particle size, temperature and impact location. Many studies have been carried out to analyse the dynamics and thermal behaviours of droplets impacting onto a cold substrate. Some authors have investigated the impact and solidification of droplets composing the resulting film and have shown that numerous parameters play a role on the droplet deposition and the structure. Leger et al. [1] have shown that in thermal spraying, substrate initial temperature and roughness play a role on the droplet impact morphology. For a low substrate temperature, the resulting splats exhibit fingering pattern whereas for a high substrate temperature, a disc shape is obtained. The consequences of the splat shapes are particular properties in the manufactured coating like structure or porosity. Scrivani et al. [2] have studied porosity and microstructure of a thick thermal barrier coating (defined by a 1 mm thickness). Their results show that coating porosity and roughness are influenced by the level of enthalpy of plasma jet. The coating porosity is linked to the efficiency of the barrier. Such a coating is used in combustion chambers to enhance the temperature and corrosion and oxidation resistances. Some numerical studies have also been carried out to model and simulate impact and solidification of a single millimetre size droplet [3]. Solidification and nonperfect thermal contact between the droplet and the substrate have been introduced, in order to improve droplet deposition processes like microcasting. Two numerical simulations and experiments have been led, with the substrate temperature below and above the droplet melting temperature. Results show that solidification affects the droplet spreading. Some authors propose the study of a limited number of droplets in various configurations, like two tin millimetre size droplets impacting one onto the other with an offset [4] or by considering a solder microdroplet pile-up [5] for which the time scale is about 100 μs. Results exhibit good agreements with experimental data and analytical expres-

* Corresponding author. Tel.: +33 (0)5 40 00 61 92; fax: +33 (0) 5 40 00 66 68.

E-mail address: lebot@enscpb.fr (C. Le Bot).

1290-0729/$ – see front matter
doi:10.1016/j.ijthermalsci.2008.08.004

Nomenclature

b	effusivity	$\mathrm{W\,s^{1/2}\,K^{-1}\,m^{-2}}$	
C	phase function		
c_p	specific heat	$\mathrm{J\,kg^{-1}\,K^{-1}}$	
e	thickness	m	
f	frequency	$\mathrm{s^{-1}}$	
f_s	solid fraction		
ρ	density	$\mathrm{kg\,m^{-3}}$	
λ	thermal conductivity	$\mathrm{W\,m^{-1}\,K^{-1}}$	
L	length	m	
L_f	latent heat of fusion	$\mathrm{J\,kg^{-1}}$	
S_C	source term	$\mathrm{W\,m^{-3}}$	
Ste	Stefan number		
t	time	s	
T	temperature	°C	
t_c	characteristic time	s	
TCR	thermal contact resistance	$\mathrm{m^2\,K\,W^{-1}}$	
x	coordinate	m	

Subscripts

sub	substrate
l	layer
a	air

Superscripts

i	initial

sions resulting from momentum and energy balances. They give information about the solidification/melting behaviour of droplets before the coating is totally manufactured. But some numerical difficulties occur while simulating impact of several droplets: fluid flow, heat transfer and interactions between particles need a large number of computational nodes to give accurate results. Simulation of droplets impact onto a cold substrate then requires large computational resources. Pawłowski [6,7] has presented a model to determine the temperature distribution in a coating created by plasma spray. They show how some parameters like the spraying distance affect the temperature distribution. Moreover, Fan et al. [8] have proposed a grid method combined to the Monte Carlo stochastic model to simulate the morphology of a composite coating during plasma spray. Results show good agreement with experiments, but heat transfers are not well rendered. Ward [9] has proposed a simple model to determine heat transfer and the coating shape during Centrifugal Spray Deposition to improve the manufacturing of ring-shaped components used in aerospace applications. The results have been compared to experimental data in terms of substrate and layers temperatures.

The aim of the present study is to propose a simple numerical model of successive depositions of several melted metal layers onto a cold substrate to simulate the evolution of cooling and solidification and potential remelting of these layers. It is useful to predict the time of process and the film solidification and to help to choose the optimum process parameters. A first approach about impact of 2D droplets has been carried out with indium samples [10]. The proposed model avoids problems due to the random character of droplet impacts and gives interesting information concerning the evolution of the coating structure. Moreover, it does not take into account problems of droplet morphology transitions, like fingering pattern, due to substrate and droplet initial temperatures [11,12]. In the present paper, we propose to study the influence of several parameters on cooling and solidification evolutions. The parameters are successively the layers thickness, initial temperatures, thermal contact resistance between layers and impact frequency. Some other experimental works have been performed to determine the solidification kinetics of indium [13]. Thus, the chosen material properties correspond to steel substrate and indium layers, as indium has a melting point at low temperature ($T_f = 156.6\,°\mathrm{C}$).

2. Numerical modelling

The aim of the present modelling is to determine how heat transfer and solidification can affect the global behaviour of several layers of melted metal impacting onto a cold substrate. It can be assumed that heat transfer characteristic time is longer than fluid flow characteristic time. So it can be considered that when a new metal melted layer impacts onto the substrate or the previous layer, flow time is negligible. This assumption allows computing only heat transfer and solidification, without convective phenomena.

The initial configuration consists in a cold substrate and a first layer. The substrate is defined by constant thermal properties λ_{sub}, $c_{p,\mathrm{sub}}$ and ρ_{sub} being respectively the thermal conductivity, the specific heat and the density, and by a thickness e_{sub}. The first melted layer is characterised by properties λ_l, $c_{p,l}$ and ρ_l and by a thickness e_l not necessarily equal to e_{sub}. Metal melted layers "appear" (impact without fluid flow) successively on the first one with a frequency noted f corresponding to a constant time between two impacts—t_c. So the term "impact" corresponds to the apparition of a new layer. Thermal properties λ_l, $c_{p,l}$ and ρ_l, and thickness e_l are here the same for all layers (which is not a restriction for the numerical tool). The domain above the last layer is constituted of air with properties λ_a, $c_{p,a}$ and ρ_a. Considering that the domain height is equal to L, air fills initially a height of $(L - e_{\mathrm{sub}} - e_l)$. Fig. 1 illustrates the physical domain at the initial time and during impact of a new layer (at t_c).

To avoid edge effects, layers are considered wide enough so that thermal transfer occurs only along the axis Ox of Fig. 1. Boundary conditions at the base of the substrate ($x = 0$) and the top of the whole domain ($x = L$) can be adapted. In the present study, only the case of an adiabatic boundary condition at the base of substrate (at the bottom) and adiabatic condition at the top of the surrounded air are considered.

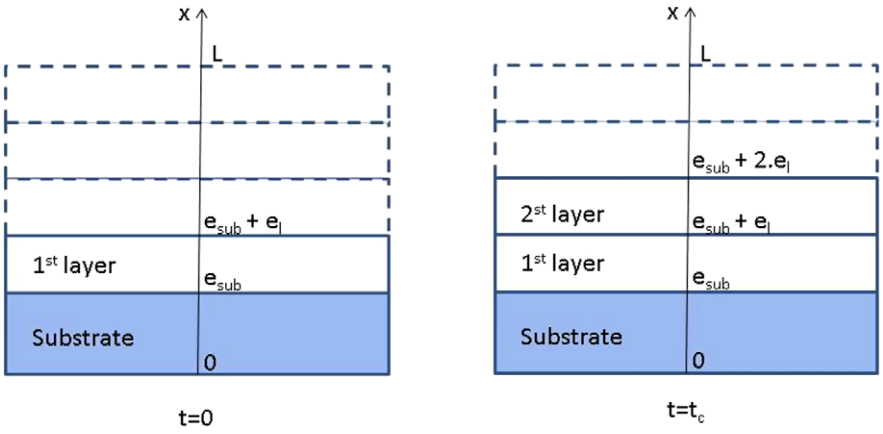

Fig. 1. Initial domain and domain at $t = t_c$.

The resolution consists in a 1D transient numerical approach. The modelling is based on the resolution of one set of equations in the whole domain:

$$\rho c_P \frac{\partial T}{\partial t} - \frac{\partial}{\partial x}\left(\lambda \frac{\partial T}{\partial x}\right) = S_C \tag{1}$$

Eq. (1) is solved with a classic finite volume method and a centered scheme is used for the spatial discretisation [14]. A second order Gear scheme is proposed for the time discretisation. The source term S_C (Eq. (6)) is solved by an iterative algorithm.

The initial conditions consist in a cold substrate and a first hot layer:

$$\begin{aligned} &T(x,0) = T_{\text{sub},i} && \text{for } 0 < x < e_s \\ &T(x,0) = T_{l,i} && \text{for } e_s < x < 2e_s \\ &T(x,0) = T_{a,i} && \text{for } 2e_s < x < L \end{aligned} \tag{2}$$

The boundary conditions are adiabatic (Dirichlet condition is also available).

$$\begin{aligned} &-\lambda_{\text{sub}} \frac{\partial T}{\partial x}\bigg|_{x=0} = 0 && \text{for } x = 0 \\ &-\lambda_a \frac{\partial T}{\partial x}\bigg|_{x=L} = 0 && \text{for } x = L \end{aligned} \tag{3}$$

To distinguish metal zones and air zones, a phase function C is introduced:

$$\begin{aligned} &C = 0 && \text{for } 0 < x < e_{\text{sub}} && \text{(substrate)} \\ &C = 1 && \text{for } e_{\text{sub}} < x < ne_l && \text{(metal layer)} \\ &C = 0 && \text{for } ne_l < x < L && \text{(air)} \end{aligned} \tag{4}$$

For the substrate zone ($0 < x < e_s$) the physical properties are fixed. For layers and air zones, thermal conductivity and specific heat exhibit a linear law:

$$\lambda(x) = C(x)\lambda_l + \big(1 - C(x)\big)\lambda_{\text{air}} \tag{5}$$

For $0 < x < e_{\text{sub}}$, thermal properties correspond to the substrate ones and correlatively $S_c = 0$ in this domain as phase change never occurs there. In the layers, properties are equal to $\lambda_l, c_{p,l}$ and ρ_l, and S_c can be different of 0 when solidification or remelting occurs. In air, $S_c = 0$ as air is never concerned with phase change. At time nt_c (where n is an integer), a $(n+1)$th layer "appears" above the previous one (at coordinates $e_{\text{sub}} + (n-1)e_l < x < e_{\text{sub}} + ne_l$). In order to update the presence of metal, and then the corresponding characteristics, the phase function, which was equal to 0 (air) in this region, is then set to 1 to indicate that the medium is now a metal layer. Thermal properties are consequently altered following Eq. (5). In the same time, S_c can become different than 0. Thanks to this method, layers can be added without changing the domain size and boundary conditions.

The source term S_c represents the energy absorbed or released during phase change. It is also expressed as a function of solid fraction f_s:

$$S_C = \rho L_f \frac{\partial f_s}{\partial t} \tag{6}$$

The solid fraction f_s is equal to 1 if metal is solid and 0 if liquid. Solidification occurs in a cell where $0 < f_s < 1$. The variable L_f corresponds to the latent heat. The source term S_c is activated only if $C = 1$, at mesh nodes containing metal. It ensures that the substrate and air cannot freeze or melt. This source term is computed by using a fixed point algorithm proposed by Voller [15]. This method has been adapted for the present study and has been already validated [16]. The employed method is useful in this case as both solidification and remelting can be computed.

It has been observed that the contact is not perfect, due to the roughness of the surface and air entrapped during deposition of melted metal [16]. The quality of the contact between two successive layers or between substrate and the first layer can influence the time evolution of solidification. In the present numerical approach, it is modelled by a thermal contact resistance. It is supposed to be constant and has the same value between two layers and between substrate and the first layer. In the numerical code, thermal conductivity is defined between two neighbouring temperature nodes. The interface between two layers or the first layer and the substrate is also defined between two temperature nodes to correspond to a conductivity node (Fig. 2). To model a nonperfect thermal contact, the thermal conductivity at the interface between two components

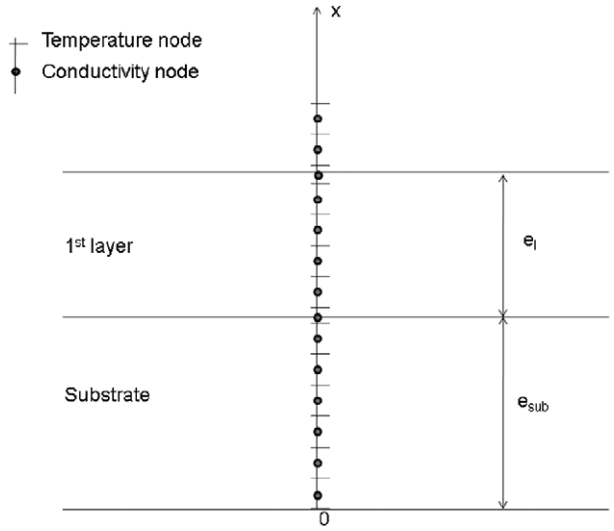

Fig. 2. Scheme of the meshgrid.

is locally modified by taking into account the thermal contact resistance TCR:

$$\lambda = \frac{x_1 + x_2}{\frac{x_1}{\lambda_1} + \mathrm{TCR} + \frac{x_2}{\lambda_2}} \tag{7}$$

Subscripts 1 and 2 correspond to two different media, x_1 and x_2 are the distances from the interface to the closest nodes in each medium (Fig. 3(a)). The advantage of this modelling is to take into account the thermal contact resistance easily and to have two different temperatures at media interfaces.

The mesh grid size is refined at interfaces of neighbouring layers where nodes are close enough to ensure that the thermal contact resistance is well rendered (Fig. 3(b)).

The thermal contact resistance model supposes that the interface thickness is equal to 0. To fit as well as possible this definition, it is practically chosen to be:

$$\Delta x_{\mathrm{TCR}} = x_1 + x_2 = \frac{\Delta x}{1000} \tag{8}$$

For millimetre thick layers, it corresponds to $\Delta x_{\mathrm{TCR}} = 10^{-6}$ m.

3. Validation and results

Prediction of evolution of the solidification front is a relatively hard task because of the source term corresponding to phase change. No analytical solution is available concerning the solidification and temperature evolutions of the contact of several successive layers. To ensure that our code is consistent with physical behaviours, validations have been carried out with a simplified configuration similar to our problem. Loulou [17] proposed an analytical solution about temperature field of two semi-infinite media suddenly in contact, one undergoing solidification, and without thermal contact resistance. In particular, the interface temperature T_{int} is expressed by:

$$T_{\mathrm{int}} = \frac{T_f b_l + T^i_{\mathrm{sub}} b_{\mathrm{sub}} \operatorname{erf}(\xi)}{b_l + b_{\mathrm{sub}} \operatorname{erf}(\xi)} \tag{9}$$

The parameter called ξ is the solution of the transcendental equation (provided that liquid and solid phases have the same conductivity, density and specific heat):

$$\frac{\exp(-\xi^2)}{\exp(\xi)} + \frac{T_f - T^i_l}{T_f - T_{\mathrm{int}}} \frac{\exp(-\xi^2)}{\operatorname{erfc}(\xi)} = \frac{\xi L_f \sqrt{\pi}}{c_P (T_f - T_{\mathrm{int}})} \tag{10}$$

Parameters b_l and b_{sub} are respectively the layer and the substrate effusivities defined by $b = \sqrt{\lambda \rho c_P}$, and L_f is the latent heat.

Thicknesses of the substrate and the layer in the computational domain are set equal to $e = 1$ m, which is wide enough to ensure a consistent solution: during a short time, the two media can be considered as semi-infinite. Each layer and substrate is composed of 100 meshes. The thermal contact is perfect (TCR = 0) and the substrate and layer initial temperatures are respectively $T^i_{\mathrm{sub}} = 25\,^{\circ}\mathrm{C}$ and $T^i_l = 190\,^{\circ}\mathrm{C}$. Thermal properties of the substrate and the layer are reported in Table 1 and are chosen representative to physical characteristics of steel and indium.

Under these assumptions and considering these data, the analytical interface temperature is computed and compared to Eqs. (9) and (10). Globally, the theoretical interface temperature gives a value $T_{\mathrm{int}} = 137\,^{\circ}\mathrm{C}$. By numerical simulation, the interface temperatures in the substrate and in the layer are equal

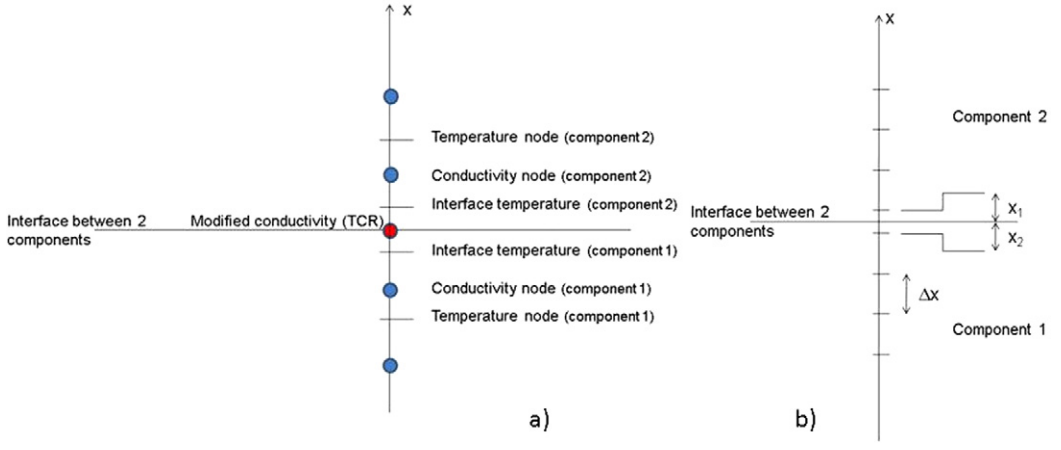

Fig. 3. Front solidification position versus time for $e_s = e_l = 1$ mm.

Table 1
Physical properties of materials

Medium	Conductivity ($W\,m^{-1}\,K^{-1}$)	Density ($kg\,m^{-3}$)	Specific heat ($J\,kg^{-1}\,K^{-1}$)	Melting temperature (°C)	Latent heat ($J\,kg^{-1}$)
Substrate (steel)	36.5	7000	465	–	–
Layer (indium)	81	7050	233	156.6	28 600

to $T_{\text{int,num}} = 136.8\,°C$. In the layer medium (indium), the temperature decreases from 190 to 156.6 °C, where a plateau occurs due to solidification, then it decreases again until 136 °C. In Eq. (6), T_{int} is a constant because the analytical configuration assumes that solidification has already begun whereas the numerical simulation takes account for an initially totally liquid layer. This explains the small discrepancy about the interface temperature between the constant analytical value and the numerical result. But rapidly, the numerical temperature converges to the predicted value. Using different mesh sizes, a second order convergence is found.

This first test does not take into account thermal contact resistance whereas the contact plays an important role in the physical deposition of several layers. Thus, a second configuration with an analytical solution is proposed to check the consistence of the numerical model about the thermal contact resistance without phase change. Let consider two semi-infinite media (substrate and layer) without phase change with a constant thermal contact resistance. If initial temperatures of these media are respectively T^i_{sub} and T^i_l, then the interface temperatures of the two media are given by expression (11):

$$T_{\text{sub,int}} = T^i_{\text{sub}} + \left(T^i_l - T^i_{\text{sub}}\right)\frac{b_l}{b_l + b_{\text{sub}}} \times \left(-\exp\left(h^2 t\right)\operatorname{erfc}\left(h\sqrt{t}\right) + 1\right)$$

$$T_{l,\text{int}} = T^i_l - \left(T^i_l - T^i_{\text{sub}}\right)\frac{b_{\text{sub}}}{b_l + b_{\text{sub}}} \times \left(-\exp\left(h^2 t\right)\operatorname{erfc}\left(h\sqrt{t}\right) + 1\right) \quad (11)$$

In this expression, b_{sub} and b_l are respectively the substrate and the layer effusivities, and h is a constant defined by:

$$h = \frac{b_{\text{sub}} + b_l}{\text{TCR} b_{\text{sub}} b_l} \quad (12)$$

The thermal contact resistance is constant and is about 10^{-6} to $10^{-3}\ m^2\,K\,W^{-1}$, which is coherent with values of physical contact of a substrate and a metal layer [18]. Actually, during the contact between the first layer and the substrate, some studies have shown that the thermal contact resistance evolves in time [19]. But after a short time, the thermal contact resistance reaches a constant value. The assumption of a constant thermal contact resistance in the present study is then validated, compared to the time of process. To increase the accuracy, an evolving value could be proposed.

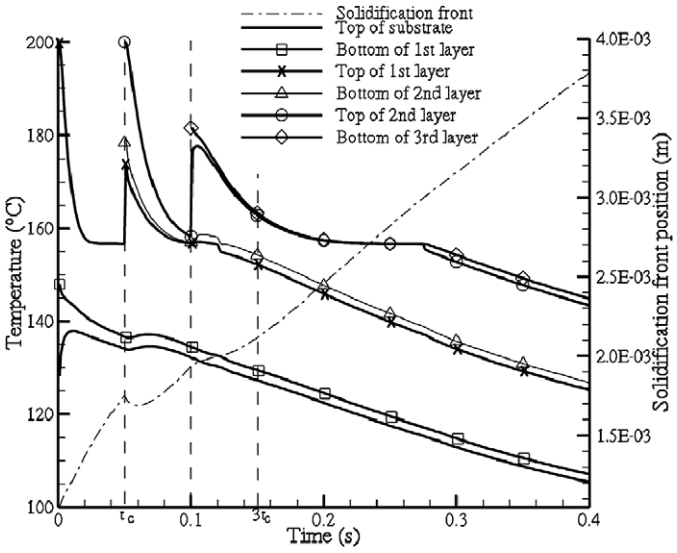

Fig. 4. Front solidification position and layers temperatures versus time.

4. Deposition of successive layers

4.1. Influence of thickness

Depending on the droplet size, the thickness of the resulting layers varies, which influences the thermal exchanges. A large droplet size corresponds to a large amount of melted metal coming in contact with the substrate or the previous droplets. Then, thick layers are considered.

Globally, results exhibit a typical behaviour (Fig. 4). Layers and substrate are both 1 mm thick, initial temperatures are respectively 25 and 200 °C for the substrate and the layers. The solidification front position increases inside the layers as they are deposited. Fig. 4 describes also the temperature evolution inside the layers and the substrate at particular location: the nodes corresponding to the top and the bottom of each layer. These temperatures will be called the "bottom temperature" and the "top temperature". In the substrate, the top temperature increases rapidly in contact with the first layer. Some slope breaks-up are noticed corresponding to the instants of deposition of next hot layers.

Concerning the first layer, the bottom temperature decreases rapidly from the initial value to the phase change temperature. Then the value remains constant during solidification and decreases until it reaches the value obtained during the sudden contact of two media with thermal contact resistance (TCR = $10^{-6}\ K\,m^2\,W^{-1}$). At $t = t_c = 0.05$ s, another layer is deposited and the first layer temperature increases. The solidification is

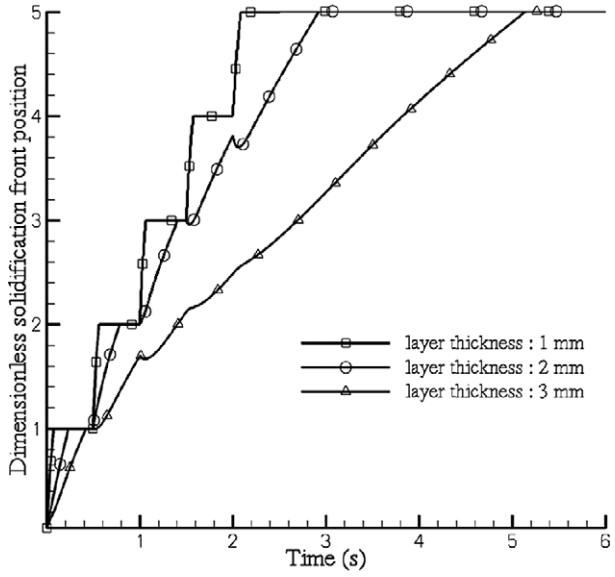

Fig. 5. Dimensionless solidification front position versus layer thickness.

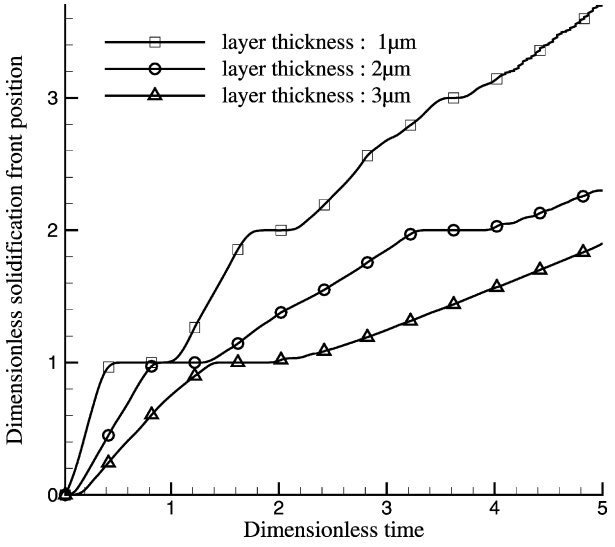

Fig. 6. Dimensionless solidification front position versus dimensionless layer thickness.

not stopped but delayed, as it can be seen in Fig. 4 at $t = 0.05$ s. Remelting occurs as a new layer brings sufficient heat to the previous one. At $t = 0.05$ s, when the second layer is deposited, the top temperature of the first layer exhibits a sudden and important increase, whereas the bottom temperature rises slowly. The increase of heat originates from the change of behaviour of the solidification evolution. For each new deposited layer $(n + 1)$, these phenomena are observed in the previous layer n.

During the deposition of several layers, the first layer is less and less influenced by the incoming of the others. Whereas the deposition of the second layer alters greatly the solidification and temperature evolutions of the first layer, the following layers less and less affect the first layer. Considering a long enough time, the first layer temperature evolution becomes independent of addition of new layers.

Several computations are carried out to determine the temperature and the solidification evolutions as a function of the layers and substrate thickness. Three simulations are carried out with layers thickness respectively equal to 1, 2 and 3 mm. Concerning the solidification evolution, for $e_l = 1$ mm, results show that the solidification front exhibits a discontinued shape due to the deposition of next layers, whereas simulations where $e_l = 2$ mm and $e_l = 3$ mm, the solidification front exhibits a smooth curve: the heat brought out from successive layers is not large enough to influence the cooling behaviour of the first layer. The study of the dimensionless front position (x/e_l) shows that when layers are thicker, the solidification needs time to reach the upper surface of each layer. It means that the solidification front exhibits a shape with fewer discontinuities than the case of thinner layers (Fig. 5). On the contrary, a thin layer allows solidification of the whole layer before impact of a next one, which can result in discontinuities in solidification front evolution and potential remelting.

The same kind of simulations has been carried out with thin micrometer layers. The characteristic time is fixed to $t_c = 5$ μs and the thermal contact resistance remains at TCR $= 10^{-6}\,\mathrm{m\,K\,m^2\,W^{-1}}$. Fig. 6 illustrates the dimensionless solidification front position (x/e_l) against dimensionless time based on the characteristic time $(t^* = t/t_c)$. Results exhibit the same behaviour than previously: for thicker layers, solidification needs a sufficiently long time to reach the upper surface.

4.2. Influence of initial temperatures

During deposition, initial temperatures of substrate and droplets play a very important role upon the structure of the final film. Several studies have shown that the substrate temperature influences the shape of the impacting droplets [18], suspected to be related to solidification. It has been found to imply a porous structure or a compact one, which corresponds in the present model to different layer properties. In the present modelling, only thermal diffusion and liquid–solid phase change are considered. Chemical behaviours like desorption due to spray conditions (and gases) are not taken into account here. These phenomena influence the cooling rate as mentioned by Leger et al. [1]. Let consider impact of 2 mm thick indium layers with an initial temperature $T_l^i = 200\,^\circ\mathrm{C}$. The initial substrate temperature is T_{sub}^i. The thermal contact resistance between two neighbouring components is TCR $= 10^{-5}\,\mathrm{K\,m^2\,W^{-1}}$ and the characteristic time is $t_c = 0.1$ s. Only three successive layers are deposited. The thermal solidification effect can be quantified by the Stefan number defined as

$$Ste = \frac{c_P(T_f - T_{\mathrm{sub}}^i)}{L_f} \tag{13}$$

Globally, for all initial substrate temperature, the general thermal behaviour is the same. The initial substrate temperatures respectively $T_{\mathrm{sub}}^i = 25\,^\circ\mathrm{C}$, $T_{\mathrm{sub}}^i = 50\,^\circ\mathrm{C}$ and $T_{\mathrm{sub}}^i = 100\,^\circ\mathrm{C}$ correspond to $Ste = 1.14$, $Ste = 0.92$ and $Ste = 0.49$. The difference between the initial substrate and layers temperatures influences the cooling rate and the solidification rate: just before the second layer impact, the substrate surface temperature is respectively $T = 127.14\,^\circ\mathrm{C}$ for $Ste = 2.25$, $T = 135.27\,^\circ\mathrm{C}$ for

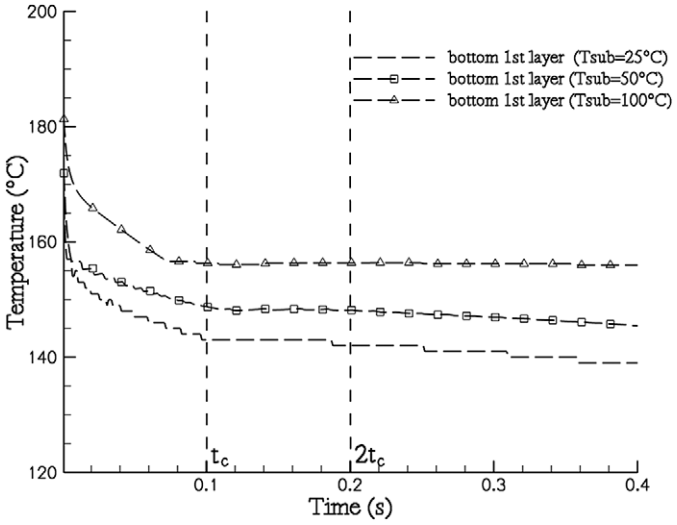

Fig. 7. Influence of the initial substrate temperature on the bottom first layer temperature.

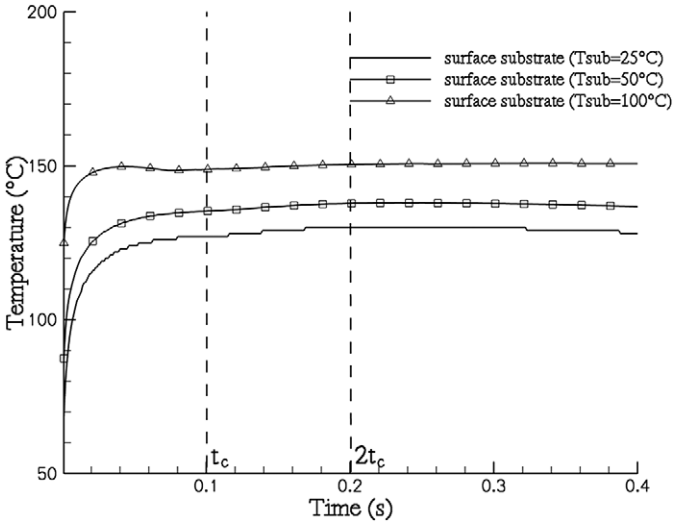

Fig. 8. Influence of the initial substrate temperature on the surface substrate temperature.

$Ste = 1.82$ and $T = 156.3\,^{\circ}\mathrm{C}$ for $Ste = 0.97$ (Fig. 8). It means that substrate superheating is higher when *Ste* is lower. In the same way, the layer cooling is quicker for high *Ste* as the layer comes in contact with a colder initial substrate (Fig. 7). It means that solidification of each layer occurs earlier.

4.3. Influence of thermal contact resistance

During deposition of droplets or thermal spraying for manufacturing metal coatings, droplets exhibit various morphologies due to initial temperatures. It can result in a splat or fragmented particles on rough substrates, leading to various coating porosities and qualities of contact [11]. Moreover, spray gases, surface chemistry of a metal substrate are influent parameters in the contact quality. Consequently, heat transfers depend on the contact state and are estimated through a thermal contact resistance. A large thermal contact resistance maintains the droplet to a high temperature, even close to the substrate. This behaviour can alter the sticking of the resulting film to the substrate or its roughness. With a bad contact, the layer temperature remains high, whereas a good contact allows a better cooling of the melted metal and subsequently, the solidification front rises faster. To take into account this phenomenon, a constant thermal contact resistance is introduced in our 1D model between the substrate and the first layer and between two successive layers. McDonald et al. [20] have experimentally and analytically studied the influence of the thermal contact resistance on cooling rate of impacting yttria-stabilised zirconia and molybdenum microdroplets. They have shown that the thermal contact resistance value has an effect on cooling rate of impacting droplets. In our study, simulations are carried out for three layers of 2 mm thickness, with an initial temperature $T = 200\,^{\circ}\mathrm{C}$. The substrate is 2 mm thick and initially at $25\,^{\circ}\mathrm{C}$. The characteristic time is set at $t_c = 0.1$ s. Several thermal contact resistances are proposed between 10^{-15} and $10^{-3}\ \mathrm{K\,m^2\,W^{-1}}$. For a high thermal contact resistance (Fig. 9), the substrate temperature remains at a low value, and the first layer temperature decreases slowly. Consequently, the successive layers contacting the hot first layer stay at $200\,^{\circ}\mathrm{C}$. For a lower thermal contact resistance, the substrate heats more and the layers cooling rate increases (Figs. 10 and 11). It implies various solidification front evolutions following the thermal contact resistance value (Fig. 12). For $\mathrm{TCR} = 10^{-3}\ \mathrm{m^2\,K\,W^{-1}}$, the results are not plotted as it stays at 0 (no solidification). The influence of the second layer appears on the solidification front from $\mathrm{TCR} = 0$ to $\mathrm{TCR} = 10^{-5}\ \mathrm{m^2\,K\,W^{-1}}$, as a slight remelting occurs. Therefore, the thermal contact has an influence on the solidification evolution. For a bad contact, the layers freeze hardly, and may remain hot. On the contrary, a very good contact implies a rapid solidification, and impact of new thin layers may provoke remelting, which can be useful to evacuate air traps.

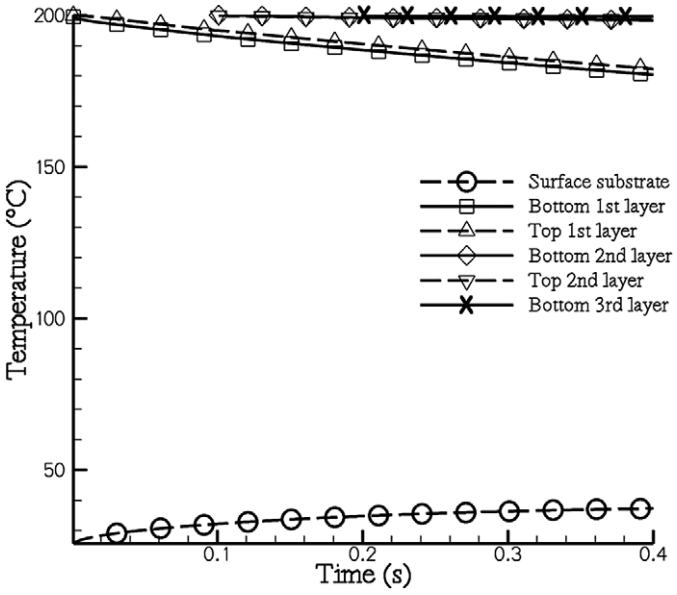

Fig. 9. Temperatures for $\mathrm{TCR} = 10^{-3}\ \mathrm{K\,m^2\,W^{-1}}$.

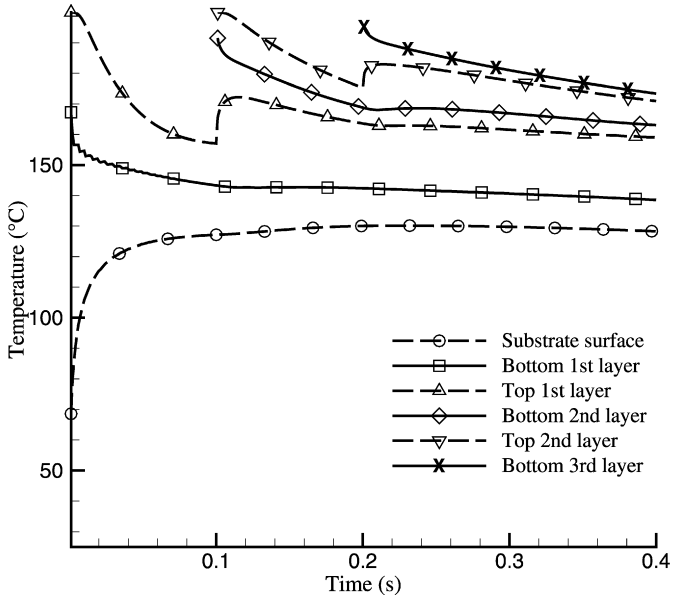

Fig. 10. Temperatures for TCR = 10^{-5} K m^2 W^{-1}.

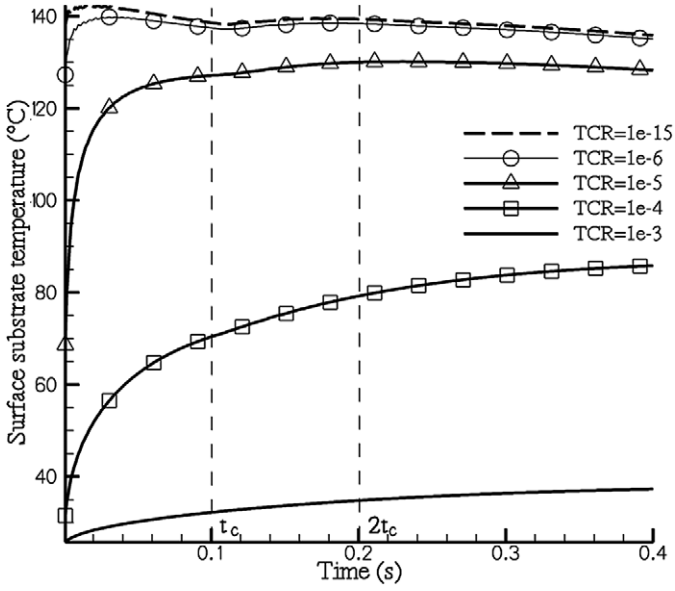

Fig. 11. Influence of thermal contact resistance on substrate surface temperature.

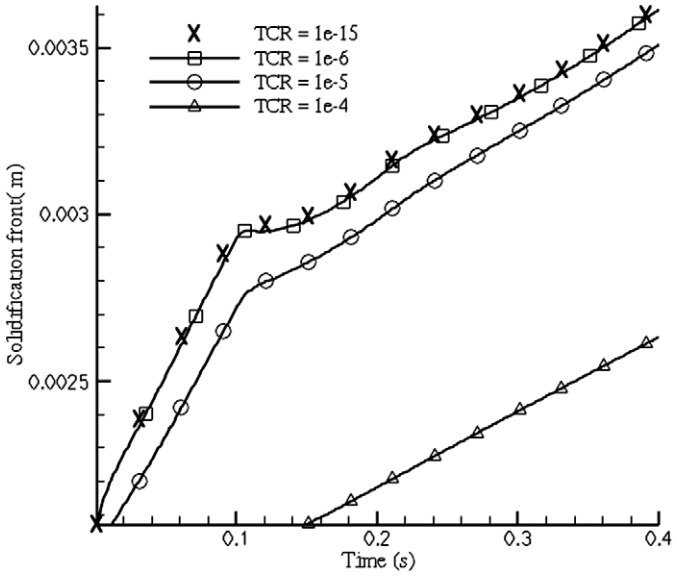

Fig. 12. Influence of thermal contact resistance on solidification front.

4.4. Influence of impact frequency

To ensure a homogeneous coating, the sprayed metal must cover the substrate with a minimal thickness. To reach this property, droplets are sprayed during a long enough period of time. Some droplets reach directly the substrate whereas some of them are deposited on the previous impacted droplets. The flow rate necessary to obtain a given thickness can be interpreted as an impact frequency of metal layers. Like droplets, layers bring heat and alter the thermal evolution of the coating and the substrate. Simulations are carried out for six layers of 2 mm thickness, with an initial temperature $T_l^i = 200\,^\circ$C. The substrate is 2 mm thick and initially at 25 °C. The thermal contact resistance is TCR = 10^{-5} m^2 K W^{-1} and the impact frequency is defined through the characteristic time t_c. Different values from $t_c = 5 \times 10^{-2}$ s to $t_c = 1$ s are proposed. For $t_c = 5 \times 10^{-2}$ s, results show a low solidification rate, as the system could be considered as a continuous supply of material and heat. On the contrary, a long enough characteristic time ($t_c = 1$ s) allows total layers solidification, but implies a local shallow remelting of the previous layer. Fig. 13 illustrates the first layer interface temperature and the solidification front position versus a dimensionless time $t_{ad} = t/t_c$. $t_{ad} = 1$ corresponds to the moment of impact of the second layer, whatever t_c is. When t_c increases, the solidification front reaches faster high values, since heat is brought out by new layers quite late. But it implies a potential remelting if layers temperature is not low enough. In the same way, the first layer temperature is widely perturbed if t_c is high, corresponding to a discontinued heat supply, whereas a short characteristic time t_c leads to a slight layer cooling. Even with a long time t_c, the layer temperature is less and less perturbed by impact of other layers which means that the first layer depositions have influence on the substrate–first layer contact. It can be useful to melt some zones where air traps have been made, as air bubbles may escape the system.

4.5. Conclusion

The coating manufacturing by droplets spraying is a complex process as thermal and dynamics behaviours interact. The structure of the resulting film depends on several parameters linked to initial temperatures and flow rate. This morphology can be understood by neglecting flow dynamics and considering deposition of successive melted metal layers on a cold substrate. We have used a simplified 1D numerical model to study thermal behaviour and solidification during deposition of several layers in order to analyse the time evolution of temperature and corresponding solidification front position. Several parameters influence the thermal behaviour, like components thickness, initial temperatures, thermal contact resistance or im-

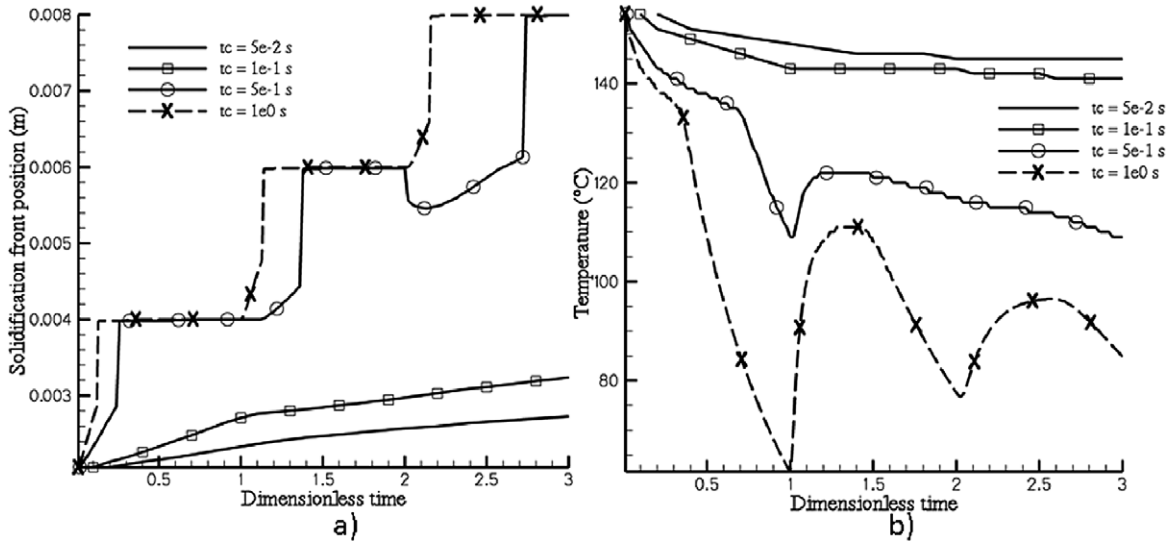

Fig. 13. Solidification front and substrate/1st layer interface temperature evolutions.

pact frequency. They define the heat supply and the potential solidification melting cycle of the created metal thin film. This approach is useful as it requires small CPU time and memory. Results have shown that spray conditions have an influence on the temperature field, solidification and remelting behaviours and consequently on the thin coating structure.

References

[1] A.C. Leger, M. Vardelle, A. Vardelle, P. Fauchais, S. Sampath, C.C. Berndt, H. Herman, Plasma sprayed zirconia: Relationship between particle parameters, splat formation and deposit generation. Part I: Impact and solidification, Journal of Thermal Spray: Practical Solutions for Engineering Problems (1996) 623–626.

[2] A. Scrivani, G. Rizzi, C.C. Berndt, Enhanced thick thermal barrier coatings that exhibit varying porosity, Materials Science and Engineering A 476 (2008) 1–7.

[3] M. Pasandideh-Fard, R. Bhola, S. Chandra, J.D. Mostaghimi, Deposition of tin droplets on a steel plate: simulations and experiments, Int. J. Heat Mass Transfer 41 (1998) 2929–2945.

[4] R. Ghafouri-Azar, S. Shakeri, S. Chandra, J. Mostaghimi, Interactions between molten metal droplets impinging on a solid surface, Int. J. Heat. Mass Transfer 46 (2003) 1395–1407.

[5] S. Haferl, D. Poulikakos, Experimental investigation of the transient impact fluid dynamics and solidification of a molten microdroplet pile-up, Int. J. Heat. Mass Transfer 46 (2003) 535–550.

[6] L. Pawłowski, M. Vardelle, P. Fauchais, A model of the temperature distribution in an alumina coating during plasma spraying, Thin Solid Films 94 (1982) 307–319.

[7] L. Pawłowski, Temperature distribution in plasma-sprayed coating, Thin Solid Films 81 (1981) 79–88.

[8] Q. Fan, L. Wang, F. Wang, Q. Wang, Modeling in composite coatings in plasma spraying, Surface & Coatings Technology 201 (2007) 6977–6984.

[9] R.M. Ward, M.D. Barratt, M.H. Jacobs, A.L. Dowson, A simple transient numerical model for heat transfer and shape evolution during the production of rings by centrifugal spray deposition, in: Proceedings of the 2003 International Symposium on Liquid Metal Processing and Casting, Nancy, France, September 21–24, 2003, pp. 223–232.

[10] C. Le Bot, Impact et solidification de gouttes métalliques sur un substrat solide, PhD Thesis, University Bordeaux 1, France 2003.

[11] S. Sampath, X.Y. Jiang, J. Matejicek, A.C. Leger, A. Vardelle, Substrate temperature effects on splat formation, microstructure development and properties of plasma sprayed coatings, Part I: Case study for partially stabilized zirconia, Materials Science and Engineering A 272 (1999) 181–188.

[12] X.Y. Jiang, J. Matejicek, S. Sampath, Substrate temperature effects on splat formation, microstructure development and properties of plasma sprayed coatings, Part II: Case study for molybdenum, Materials Science and Engineering A 272 (1999) 189–198.

[13] C. Le Bot, D. Delaunay, Rapid solidification of indium: Modeling subcooling, Materials Characterization 59 (5) (2008) 519–527.

[14] S.V. Patankar, Numerical Heat Transfer and Fluid Flow, Hemisphere Publishing Corporation, New York, 1990.

[15] V.R. Voller, Fast implicit finite-difference method for the analysis of phase change problems, Numerical Heat Transfer, Part B 17 (1990) 155–169.

[16] C. Le Bot, S. Vincent, E. Arquis, Impact and solidification of indium droplets on a cold substrate, Int. J. Thermal Sciences 44 (2005) 219–233.

[17] T. Loulou, D. Delaunay, The interface temperature of two suddenly contacting bodies, one of them undergoing phase change, technical note, Int. J. Heat Mass Transfer 40 (1997) 1713–1716.

[18] M. Vardelle, A. Vardelle, A.C. Leger, P. Fauchais, D. Gobin, Influence of particle parameters at impact on splat formation and solidification in plasma spraying processes, Journal of Thermal Spray Technology 4 (1) (1994) 50–58.

[19] T. Loulou, E.A. Artyukhin, J.-P. Bardon, Estimation of thermal contact resistance during the first stages of metal solidification process: II. Experimental setup and results, Int. J. Heat Mass Transfer 42 (12) (1999) 2129–2142.

[20] A. McDonald, C. Moreau, S. Chandra, Thermal contact resistance between plasma-sprayed particles and flat surfaces, Int. J. Heat Mass Transfer 50 (2007) 1737–1749.